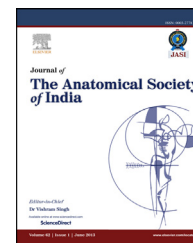


Available online at www.sciencedirect.com

ScienceDirect

journal homepage: www.elsevier.com/locate/jasi

Original Article

Morphology of the olfactory fossa – A new look

Tony George Jacob^{a,*}, J.M. Kaul^b^a Assistant Professor, Department of Anatomy, Vardhman Mahavir Medical College and Safdarjung Hospital, New Delhi 110029, India^b Director Professor, Department of Anatomy, Maulana Azad Medical College, Bahadur Shah Zafar Marg, New Delhi 110029, India

ARTICLE INFO

Article history:

Received 22 December 2013

Accepted 10 April 2014

Available online 9 May 2014

Keywords:

Ethmoid

Endoscopy

Cribriform plate

Fovea ethmoidalis

Morphometry

ABSTRACT

Introduction: The olfactory fossa is a depression in the anterior cranial cavity whose floor is the cribriform plate of the ethmoid bone. This delicate bony plate separates the anterior cranial fossa from the nasal cavity.

Methods: We studied the morphology of the olfactory fossa in 32 dry skulls, derived from North India, of undetermined sex, using a hydroxyphilic siloxane based gel. Molds of the olfactory fossa and adjacent cranial fossa were made and measurements of length, width, depth and angle of embankment (angle between the lateral wall of the olfactory fossa and the medial part of the anterior cranial fossa) were done on them and their coronal sections.

Results: The average length of the olfactory fossa was 2.11 cm. The average width was 0.39 cm and the mean angle of embankment was 130.5°. According to the measured depth, the incidence of Keros' type I (1–3mm) was 23.44%, type II (4–7mm) – 70.83% and type III (8–16mm) – 5.73%. Type III was more frequent on the left side. The fossa in north India is deeper in the middle than its anterior and posterior ends. It had a narrow anterior and broad posterior end (54.69%). There were no overall significant differences between the right and left side for the various morphometric parameters.

Discussion: This study provides baseline morphometric data of the olfactory fossa in the North Indian population and this knowledge may help the radiologists to analyze scans of this region and minimize complications associated with surgeries in this delicate area.

Copyright © 2014, Anatomical Society of India. Published by Reed Elsevier India Pvt. Ltd. All rights reserved.

1. Introduction

Functional endoscopic sinus surgery (FESS) has become a common modality of treatment for disorders of the nose and paranasal sinuses. Prior knowledge of the anatomy of the

paranasal sinuses, anterior skull base and olfactory zone is necessary for good results.^{1,2}

The ethmoid is a complex and delicate bone that lies in the midline of the facial skeleton. It is the key bone in FESS.³ It consists of a midline perpendicular plate and crista galli and two lateral labyrinths of air cells connected to each other

* Corresponding author.

E-mail address: tonygeorgejacob@gmail.com (T.G. Jacob).<http://dx.doi.org/10.1016/j.jasi.2014.04.006>

0003-2778/Copyright © 2014, Anatomical Society of India. Published by Reed Elsevier India Pvt. Ltd. All rights reserved.

superiorly by the cribriform plate. The labyrinths are covered laterally by the lamina papyracea in the medial wall of the orbit. The roof of the ethmoid labyrinth is formed medially by the cribriform plate and the lateral lamina and laterally by the portion of the frontal bone that covers and closes the ethmoid cells superiorly – the fovea ethmoidalis.^{4–7} The levels of the ethmoid roof and cribriform plate can vary even in the same person; depending on the vertical extent of the lateral lamina. The olfactory fossa (OF) is the thinnest and an extremely variable part of the anterior skull base. After the analysis of 450 cadaveric skulls Keros noted three main forms of the OF, depending on the level of the ethmoid roof. Keros type I characterizes the depth of the OF to be 1–3 mm; type II – 4–7 mm and type III – 8–16 mm. Keros type III is called ‘dangerous ethmoid’ due to the high incidence of complications associated with its presence during surgeries in this region.^{8–10} In Keros’ III, the OF is deeper and the bone is thin. Keros’ classification provides an objective assessment of anterior skull base anatomy and can therefore guide the surgeon to the superior bony extent of the medial orbital wall during orbital decompression.¹¹ Keros also has described the width of the ethmoid labyrinth and OF at different points. He noted that there is a gradual enlargement of its width posteriorly.⁹

Preoperative imaging helps in identifying the marginal thickness of the cribriform plate, various anatomical variants of the OF and the variable width of the cribriform plate in the anterior and posterior third. Imaging modalities like Computerised Tomographic (CT) scans and Digital Volume Tomography (DVT) can evaluate the bony configuration of the OF. Good attention to the anatomy of this region would help in preventing serious consequences such as CSF rhinorrhoea, meningitis, anosmia and brain abscesses.⁹ It has been shown that 30.1% of CSF leaks are due to iatrogenic causes.¹²

To the best of our knowledge, there are no anatomic studies of the OF in the North Indian population. Therefore, we planned this project to study the morphology of the olfactory fossa in dry skulls using a hydroxyphilic siloxane gel that can set and reproduce the form of the area without any distortion.¹³

We hope that this study would help the Indian endoscopic surgeon and the radiologist by providing the baseline morphometric information regarding the OF. This would also be a method to replicate in studies that need to assess the volumes of regions that are difficult to access anatomically, without distortions and without damaging the anatomical specimens that are in short supply today, especially because research in surgical anatomy is becoming more and more important.

2. Materials and methods

The study was conducted on thirty-two dry skull bases of undetermined sex and age after obtaining clearance from the Institutional Protocol and Human Ethics Committee of Maulana Azad Medical College, New Delhi, India[#].

[†] Aquasil LV was provided free of cost by Dentsply, India for this work.

[#] The dry skulls were from the bone collection at the Department of Anatomy, Maulana Azad Medical College, New Delhi, India.

Initially, the skulls were studied for the general shape and form of the OF and checked for any osteological deformities. Thereafter, we used a hydroxyphilic siloxane based gel (Aquasil LV – Dentsply, U.S.A.)[†] to make molds of the OF and the adjoining parts of the anterior cranial fossa. This material has been reliably used by dentists to create impressions and molds.^{13–15}

The product consists of two gels – the base and a catalyst – attached to a double-barrel injection gun that has a mixing nozzle. The gun operates in such a way that the catalyst and the base are mixed in equal quantity within the nozzle. The mixture was injected into the OF (Figs. 1 and 2), starting from the floor and ending by covering most of the crista galli and the medial part of the anterior cranial fossa. It was allowed to set for ten minutes and the casts were removed by pulling on its edges because the set product was flexible, non-adherent and retained the shape of the structure in which it was set. The various dimensions of the OF were measured on the casts as shown in Fig. 3.

First of all, we measured the length of the fossa at the base of the mold by using Vernier callipers. We then sectioned the casts into nine equal parts depending on their individual length. Therefore, there were three sections each for the anterior, middle and posterior parts. Further measurements were made on the anterior surfaces of the sections (Fig. 3). We measured the maximum width and height of the olfactory fossa using Vernier callipers on the anterior surface of the sections of the molds. The measurements were taken for each section, hence, we had three measurements of height and width for the anterior, middle and posterior thirds of the molds. The arrows indicating the dimensions measured on the mold have been shown in Fig. 3. We also traced the sections on a piece of paper, extrapolated the vertical and horizontal limbs of the lateral edges and measured the angle between them using a protractor. This represented the angle of embankment between the lateral wall of the OF and the medial part of the anterior cranial fossa.

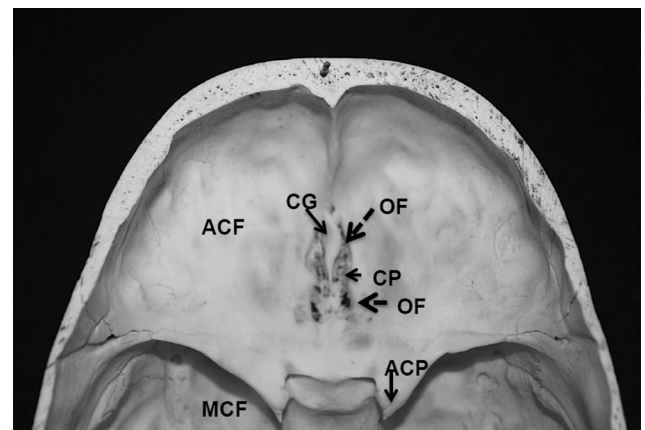


Fig. 1 – Photograph of the anterior part of the cranial cavity showing the anterior cranial fossa (ACF) and the middle cranial fossa (MCF). In the midline is the crista galli (CG) flanked by the cribriform plate of the ethmoid (CP). One can observe that the anterior end of the olfactory fossa (OF) is narrow (arrow with broken line) and its posterior end is wide.

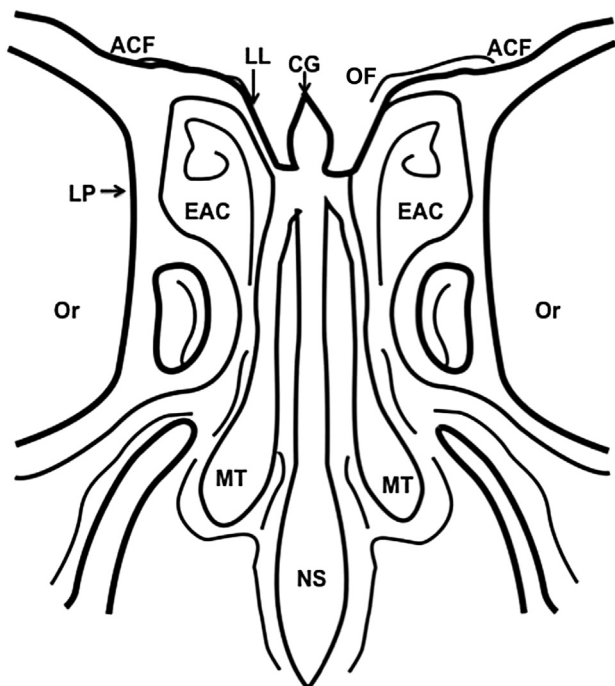


Fig. 2 – Schematic sketch of a coronal section of the skull passing through the nasal cavity showing the nasal septum (NS) in continuity with the crista galli (CG) that is flanked by the olfactory fossa (OF), which is bound laterally by the lateral lamella (LL). The lateral lamella is continuous with the root of the middle turbinate (MT). The sketch also displays the ethmoid air cells (EAC) separated by the lamina papyracea (LP) from the orbit (Or), superior to which is the anterior cranial fossa (ACF).

We also classified OF according to the Keros' classification, which is based on their depth – Keros I – 1–3 mm depth, Keros II – 4–7 mm depth and Keros III – 8–16 mm depth. Thereafter, we determined the percentage distribution of the Keros types.

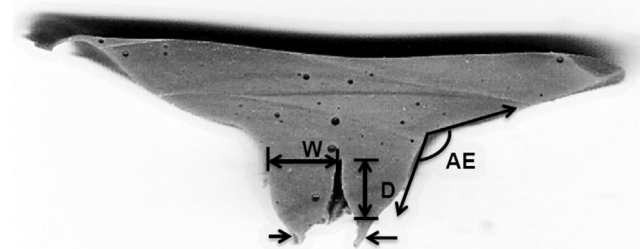


Fig. 3 – Coronal section of the mold made with Aquasil LV of the olfactory fossa showing the method of measurement of its width (W), depth (D) and the angle of embankment (AE) between the lateral lamella of the cribriform plate and the fovea ethmoidalis of the frontal bone. N.B. that the mold material has formed tails (arrow) because of it passing through the cribriform plate of the ethmoid. These tails were not included in the measurement of the depth of the olfactory fossa.

The data comprising continuous variables was represented by their mean and standard deviation. Further statistical analysis was done by using SPSS ver.16 using independent samples t-test. For categorical variables, like the distribution of the Keros types and the shape of the olfactory fossa, we used Fisher's exact test for significance. In the case of the shape of the OF, single incidences of a particular type of shape were excluded to avoid false attribution of significance to their occurrence on comparing the two sides. The overall level of significance was set at $p < 0.05$.

3. Results

The OF lies in the anteromedial part of the anterior cranial fossa and forms part of the roof of the nasal cavity. Its floor is the cribriform plate of the ethmoid, the lateral lamella binds it laterally and the crista galli lies medially.

We observed that the fossa could vary in length, depth and width within the same skull and between skulls.

We have summarised the findings of the morphometric measurements of the olfactory fossa in [Table 1](#).

There was no significant difference between the length and breadth of the OF between the right and left sides ($p > 0.05$). We also observed that as a rule (100% of cases) all olfactory fossae had shallower anterior and posterior ends when compared to the middle region ([Supplementary data](#)). It resembled a shallow trough. The data for the depth of the fossae also enabled us to classify their anterior, middle and posterior thirds according to the classification proposed by Keros (1962). The data has been summarised in [Table 2](#). Overall there were 5.73% of instances, where the skulls had the dangerous Keros' III depth of the OF and this was most frequent in the middle third of the fossa. There was significant difference between the distribution of the various Keros' types between the right and left sides in the anterior third ($p = 0.001$) ([Supplementary Table 2](#)). In the anterior third the OF were more of type I on the left side than the right, thus the fossae were shallower on the left side. In the middle region, there were more number of type II OF on the right side but the incidence of the dangerous type III fossae were more numerous on the left side ($p = 0.003$) ([Supplementary Table 3](#)).

Table 1 – Morphometry of olfactory fossa.

		Left	Right	Mean	p-value
Depth (cm)	Ant	0.43 (0.18)	0.45 (0.15)	0.49	0.655
	Mid	0.57 (0.20)	0.53 (0.17)		0.431
	Post	0.48 (0.13)	0.48 (0.11)		0.917
Width (cm)	Ant	0.27 (0.20)	0.30 (0.19)	0.39	0.527
	Mid	0.39 (0.19)	0.44 (0.18)		0.344
	Post	0.46 (0.10)	0.47 (0.10)		0.772
Angle (°)	Ant	130.08 (12.26)	128.89 (11.09)	130.5°	0.683
	Mid	128.74 (14.66)	130.58 (13.14)		0.598
	Post	133.10 (12.20)	131.59 (12.71)		0.629
Length (cm)		2.09 (0.36)	2.13 (0.34)	2.11	0.67

Summary of morphometric data of the left and right OF. There was no significant difference between the sides for any of the parameters (Ant – anterior, Mid – middle, Post – posterior).

Table 2 – Keros' types in different regions of the OF.

Keros' type	Left				Right				Overall	
	Ant	Mid	Pos	%	Ant	Mid	Pos	%	Average	%
I	12.00	6.00	6.00	25.00	9.00	4.00	8.00	21.88	7.50	23.44
II	19.00	20.00	26.00	67.71	22.00	25.00	24.00	73.96	22.67	70.83
III	1.00	6.00	0.00	7.29	1.00	3.00	0.00	4.17	1.83	5.73

Percentage distribution of the Keros' types in the anterior (Ant), middle (Mid) and posterior (Pos) thirds of the OF.

However, there was no difference between the two sides in the posterior region of the olfactory fossa ($p = 0.625$) (Supplementary Table 4), but we also noted that the posterior region had a zero incidence of the Keros' type III. When we compared the sums of the various Keros types in the anterior, middle and posterior regions of the fossae, we found a significant difference between the two sides ($p = 0.018$) (Supplementary Table 5). The OF were shallower on the right side, and the left side also had a greater incidence of the dangerous (deeper) variety of Keros' types, as was also noticed when we analysed the three regions separately.

The width of the OF ranged from 0.1 to 1.3 cm. There was no significant difference in the width on the left and right sides ($p > 0.05$) (Table 1). With regard to the width we noticed there were different forms of the OF that determined its form in three dimensions. We determined the shape of the fossae according to its width in the anterior, middle and posterior thirds. The most common shape was that of a narrow anterior end and a broad posterior end (<<<, 54.69%). The findings are summarised in Table 3. We compared the distribution of the first four types of shapes and found that there was a significant difference between the left and right sides. The narrow anterior end and broad posterior end (<<<) was more common on the right side, the narrow anterior end and subsequently parallel sides (<==) was more common on the left side ($p = 0.033$) (Supplementary Table 6).

The angle of embankment of the lateral wall of the OF ranged from 90° to 170°. The overall angle of embankment was

130.5°. There was no significant difference in the angulation of the left or right sides ($p > 0.05$) (Table 1).

4. Discussion

Galen (130–201 A.D.) first described the ethmoid¹⁶ and Zuckerkandl, published the first detailed and systematic anatomic account of the paranasal sinuses,¹⁷ but today Functional Endoscopic Sinus Surgery (FESS), a procedure that has revolutionized the diagnosis and treatment of many problems that plague the nose and the PNS^{18,19} has made it mandatory for us to understand the anatomy of the anterior skull base.²⁰ Here, we have studied the morphology of the OF in dry skulls derived from the North Indian population.

Despite our best efforts, we did not find any literature that details the length, width or angle of embankment of the OF, especially from the North Indian population. But there were numerous papers that specified the depth of the fossa and also classified them according to Keros.

The depth of the OF was found to be between 4 mm and 7 mm in 70.2% in Keros' study.⁸ Lang (1998) observed that the average depth was 0.50 cm.²¹ Meloni et al (1992) found that this measurement was 0.59 cm on average in 106 patients.²² Erdem et al (2004), in their study on 136 CT scans found that the average depth of the cribriform plate was 0.61 cm.²⁰ Arslan et al (1999) detected that the depth was 0.8 cm (range 0.2–1.4 cm) on the right side and of 0.95 cm (range 3–16 mm) on the left side.²³ The findings of our study are closer to those described by Keros (1962), Meloni et al (1992) and Lang (1998). The values quoted by the other studies are much higher than what we found in our study (0.49 cm). Like us, Meloni et al (1992) Lang (1998) and Erdem et al (2004) too did not find any difference in the depth of the OF between the left and right sides. The differences in the heights of the fossa may be explained by the difference in extent of pneumatization of the ethmoid labyrinth and the frontal sinus. Moreover, the lowering of the cribriform plate continues in an anteroposterior direction depending on the degree of pneumatization of the frontal sinus.²⁴ However, we found that the middle region of the OF was deeper than the anterior and posterior regions. Therefore, probably the manner of pneumatization of the frontal and ethmoid sinuses is different in the Indian population compared to other populations. A study by Giannetti et al (2012) shows that the depth of the olfactory fossa (averaging 0.6 cm on the right and left sides) was not a risk factor for primary spontaneous CSF leak,²⁵ but 30.1% of all CSF leaks are known to be iatrogenic in origin.¹² Therefore, the depth of the olfactory fossa is important to consider prior to surgeries in the region.

Table 3 – Classification and percentage distribution of the various shapes of the olfactory fossa.

Shape	Left	Right	Total	Percentage
<<<	14	21	35	54.69
<==	8	3	11	17.19
==<	4	4	8	12.50
<>	4	1	5	7.81
>>>	2	1	3	4.69
==>	0	1	1	1.56
><	0	1	1	1.56
	32	32	64	100

Percentage distribution of the various shapes of the OF, determined according to the width of the OF in the anterior, middle and posterior thirds (Shape types: <<<, narrow anterior end and broad posterior end; <==, narrow anterior end with parallel edges for the middle and posterior regions; ==<, narrow and parallel anterior and middle thirds and a broad posterior end; <>, narrow anterior and posterior ends with a broad middle; >>>, broad anterior end and narrow posterior end; ==>, parallel anterior and middle portions and a narrow posterior end; ><, broad anterior and posterior thirds with a narrow middle).

Keros, studied 450 cadaveric specimens and classified the olfactory fossae according to their depth. He found type I in 12%, type II in 70% and type III in 18%.⁸ Basak et al (1998) found the same in 14%, 58% and 28%, respectively in a CT scans based study.²⁶ The incidence of the Keros' types I, II and III were 8.1%, 59.6% and 32.3%, respectively in the study by Erdem et al (2004).²⁰ In another study on the anterior skull base done with the help of CT scans the authors found type I in 8.0%; type II in 80.3% and type III in 11.7% of patients.²⁷ A similar study by Guldner et al (2011) revealed 13% of type I, 64% of type II and 23% of type III.²⁸ Their incidence of the dangerous type III was much higher than what we found in our study (5.73%). Our finding, however, was similar to findings found by Ramakrishnan et al in the United States of America. They found that 42% of patients had type I, 50% had type II, and 8% had type III.²⁹ Our findings are also similar to one in a South Indian population, that is also CT based. They found type I in 20% of patients, type II in 78.7% and type III in 1.3% of cases.³⁰ Surprisingly, a study on Malay, Chinese and Indian ethnic groups in Malaysia revealed 0% of type III olfactory fossae in the preoperative CT scans.³¹ Anderhuber performed a similar CT based study in children between 0 and 14 years and his findings were that there were 14% of type I, 71% of type II and 15% of type III.³² It appears that the incidence of type III does not change much with age in the Caucasian populations, if we compare the studies that were performed in Germany alone, starting with Keros. Similarly, the Indian population may also have similar incidences of type III in the adult and paediatric populations. This aspect needs to be studied further.

Importantly, we found that there was an asymmetry of depth of more than 0.2 cm in 15.63% of cases (Supplementary Table 1), whereas Erdem et al (2004) found such a difference in 22.86% of cases.²⁰ Zacharek et al, (2005) in their study also found that the posterior region of the ethmoid roof is relatively constant and could be used as a reliable landmark.³³ We also found that there was no variability in the posterior ethmoid with respect to the Keros types. In addition, we found that the variability of shape and depth were more pronounced on the right side than on the left but that the dangerous type III was also more common on the left side. That the OF is asymmetric,^{10,34} especially in the anterior region is already known,³³ but we would suggest that the surgeon should be more careful while operating on the left side even though it is more variable on the right side because the incidence of type III was more common on the left.

Guldner et al (2011) measured the angle between the cribriform plate and the lateral lamella of the OF. They found the angle to be about 103.8° in the anterior ethmoid.²⁸ They did not measure this angle in the middle or posterior regions of the fossa. We have measured the angle of embankment, which is between the lateral lamella and the roof of the ethmoid, in the anterior, middle and posterior thirds of the olfactory fossa, and found it to be approximately 130°. This would determine the angle at which the endoscope would enter the anterior ethmoidal air cells during surgery.

Considering ethnic, inter-individual and intra-individual variations in the OF, paranasal sinus CT-scans taken in the coronal plane can provide adequate information about the patient's individual conditions and variations.¹⁸ Some authors

believe that it is essential to know the average length of peripheral anatomic structures to avoid serious complications that may occur during endoscopic surgeries. Diligent preoperative review of paranasal sinus CT scans in such patients, to them, is of utmost importance to prevent severe intraoperative complications.³⁵ This is also evident because recently the rate of major complications during FESS is 0.25%³⁶; whereas earlier it had been 1.41%³⁷ – an almost five times decrease in incidence. This may be due to better imaging and better training of the surgeons over the years.³⁸

5. Conclusion

To the best of our knowledge there have been no studies in any populations that detail the morphology of the OF by using a silicone based mold material. We feel that this study is significant because it could help surgeons and the radiologists to understand the anatomy of the OF in three dimensions. This may reduce some of the complications associated with endoscopic surgeries of this region.

Conflicts of interest

All authors have none to declare.

Acknowledgements

The authors would like to thank Prof. Mahesh Verma of the Maulana Azad Dental College, New Delhi, for having suggested this methodology. Special thanks to Prof. T.S. Roy for critically reviewing the paper and providing valuable suggestions.

Appendix A. Supplementary data

Supplementary data related to this article can be found at <http://dx.doi.org/10.1016/j.jasi.2014.04.006>.

REFERENCES

1. Souza SA, Souza MMA, Idagawa M, et al. Computed tomography assessment of ethmoid roof: a relevant region at risk in endoscopic sinus surgery. *Radiol Bras*. 2008;41(3):143–147.
2. Welch KC, Palmer JN. Intraoperative emergencies during endoscopic sinus surgery: CSF leak and orbital hematoma. *Otolaryngol Clin N Am*. 2008;41:581–596.
3. Chong VFH, Fan YF, Lau D, et al. Functional Endoscopic Sinus Surgery (FESS): what radiologists need to know. *Clin Radiol*. 1998;53:650–658.
4. Mosher HP. The applied anatomy and intra-nasal surgery of the ethmoidal labyrinth. *Laryngoscope*. 1913;23(9):881–907.
5. Hollinshead WH. *Anatomy for surgeons*. In: *The Head and Neck*. 3rd ed. vol. 1. Philadelphia: Harper and Row; 1956:252–253.

6. Stammberger H, Kennedy DW, Bolger WE, et al. Paranasal sinuses: anatomic terminology and nomenclature. *Ann Otol Rhinol Laryngol.* 1995;104(suppl 167):7–16.
7. Stranding S, Collins P, Healy JC, et al. Bones of the facial skeleton and cranial vault. In: Stranding S, Borley NR, Collins P, et al., eds. *Gray's Anatomy*. 40th ed. Spain: Churchill Livingstone Elsevier; 2008:472–473.
8. Keros P. On the practical value of differences in the level of the lamina cribrosa of the ethmoid. *Z Laryngol Rhinol Otol.* 1962;41:809–813.
9. Savvateeva DM, Guldner C, Murthum T, et al. Digital volume tomography (DVT) measurements of the olfactory cleft and olfactory fossa. *Acta Otolaryngol.* 2010;130:398–404.
10. Lebowitz RA, Terk A, Jacobs JB, et al. Asymmetry of the ethmoid roof: analysis using coronal CT. *Laryngoscope.* 2001;111:2122–2124.
11. Gauba V, Saleh GM, Dua G, et al. Radiological classification of anterior skull base anatomy prior to performing medial orbital wall decompression. *Orbit.* 2006;25:93–96.
12. Psaltis AJ, Schlosser RJ, Banks CA, et al. A systematic review of the endoscopic repair of cerebrospinal fluid leaks. *Otolaryngol Head Neck Surg.* 2012;147:196–203.
13. Perakis N, Urs CB, Pascal M. Final impressions: a review of material properties and description of a current technique. *Int J Periodontics Restorative Dent.* 2004;24:109–117.
14. Berg JC, Glen HJ, Xavier L, et al. Temperature effects on the rheological properties of current polyether and polysiloxane impression materials during setting. *J Prosthet Dent.* 2003;90:150–161.
15. Rudolph H, Sebastian Q, Manuela H, et al. Randomized controlled clinical trial on the three-dimensional accuracy of fast-set impression materials. *Clin Oral Investig.* 2013;17:1397–1406.
16. Blanton PL, Biggs NL. Eighteen hundred years of controversy: the paranasal sinuses. *Am J Anat.* 1969;124:135–148.
17. Marquez S, Lawson W, Schaeffer SD, et al. Anatomy of the nasal accessory sinuses. In: Wackym PA, Rice DH, Schaeffer SD, eds. *Minimally Invasive Surgery of the Head, Neck and Cranial Base*. Philadelphia: Lippincott, Williams and Wilkins; 2002:153.
18. Stammberger H. *Functional Endoscopic Sinus Surgery*. Philadelphia: BC Decker; 1991:17–60.
19. Mafee MF, Chow JM, Meyers R. Functional endoscopic sinus surgery: anatomy, CT screening, indications and complications. *AJR.* 1993;160:735–744.
20. Erdem G, Erdem T, Miman MC, et al. A radiological anatomy of the cribriform plate compared with constant structures. *Rhinology.* 2004;42:225–229.
21. Lang J. *Klinische Anatomie der Nase, Nasenhöhle und Nebenhöhlen*. New York: Grundlagen für Diagnostik und Operation. Thieme Stuttgart; 1998:23–27.
22. Meloni F, Mini R, Rovasio S, et al. Anatomic variations of surgical importance in ethmoid labyrinth and sphenoid sinus. A study of radiologic anatomy. *Surg Radiol Anat.* 1992;14:65–70.
23. Arslan H, Aydynlyoglu A, Bozkurt M, et al. Anatomic variations of the paranasal sinuses: CT examination for endoscopic sinus surgery. *Auris Nasus Larynx.* 1999;26:39–48.
24. Krmptotic-Nemanic J, Vinter I, Judas M. Transformation of the shape of the ethmoid bone during the course of life. *Eur Arch Otorhinolaryngol.* 1997;254:347–349.
25. Giannetti AV, Guimarães RES, Santiago APMS, et al. A tomographic study of the skull base in primary spontaneous cerebrospinal fluid leaks. *Neuroradiology.* 2012;54:459–466.
26. Basak S, Karaman CZ, Akdilli A, et al. Evaluation of some important anatomical variations and dangerous areas of the paranasal sinuses by CT for safer endonasal surgery. *Rhinology.* 1998;36:162–167.
27. Leunig A, Betz CS, Sommer B, et al. Anatomic variations of the sinuses; multiplanar CT-analysis in 641 patients. *Laryngorhinootologie.* 2008;87:482–485.
28. Guldner C, Diogo I, Windfuhr J, et al. Analysis of the fossa olfactoria using cone beam tomography (CBT). *Acta Otolaryngol.* 2011;131:72–78.
29. Ramakrishnan VR, Suh JD, Kennedy DW. Ethmoid skull-base height: a clinically relevant method of evaluation. *Int Forum Allergy Rhinol.* 2011;1:396–400.
30. Ali A, Kurien M, Shyamkumar NK, et al. Anterior skull base: high risk areas in endoscopic sinus surgery in chronic rhinosinusitis – a computed tomographic analysis. *Indian J Otolaryngol Head Neck Surg.* 2005;57:5–8.
31. Alazzawi S, Omar R, Rahmat K, et al. Radiological analysis of the ethmoid roof in the Malaysian population. *Auris Nasus Larynx.* 2012;39:393–396.
32. Anderhuber W, Walch C, Fock C. Configuration of the ethmoid roof in children 0–14 years of age. *Laryngorhinootologie.* 2001;80:509–511.
33. Zacharek MA, Han JK, Allen R, et al. Sagittal and coronal dimensions of the ethmoid roof: a radio anatomic study. *Am J Rhinol.* 2005;19:348–352.
34. Rieb M, Rieb G. Height of right and left ethmoid roofs: aspects of laterality in 644 patients. *Int J Otolaryngol.* 2011. <http://dx.doi.org/10.1155/2011/508907>. Article ID 508907, 4pp.
35. Guler C, Uysal IO, Salk PKI, et al. Analysis of ethmoid roof and skull base with coronal section paranasal sinus computed tomography. *J Craniofacial Surg.* 2012;23:1460–1464.
36. Sharp HR, Crutchfield L, Rowe-Jones JM, et al. Major complications and consent prior to endoscopic sinus surgery. *Clin Otolaryngol Allied Sci.* 2001;26:33–38.
37. Harkness P, Brown P, Fowler S, et al. A national audit of sinus surgery. Results of the Royal College of Surgeons of England comparative audit of ENT surgery. *Clin Otolaryngol Allied Sci.* 1997;22:147–151.
38. Siedek V, Pilzweiger E, Betz C, et al. Complications in endonasal sinus surgery: a 5-year retrospective study of 2,596 patients. *Eur Arch Otorhinolaryngol.* 2013;270:141–148.